Quantum Monte Carlo Calculations of $A \leq 6$ Nuclei

B. S. Pudliner and V. R. Pandharipande
Physics Department, University of Illinois at Urbana-Champaign, 1110 West Green Street, Urbana, Illinois 61801

J. Carlson
Theoretical Division, Los Alamos National Laboratory, Los Alamos, New Mexico 87545

R. B. Wiringa
Physics Division, Argonne National Laboratory, Argonne, Illinois 60439
(Received 11 January 1995)

The energies of ^{3}H, ^{3}He, and ^{4}He ground states, the $\frac{3}{2}^-$ and $\frac{1}{2}^-$ scattering states of ^{5}He, the ground states of ^{6}He, ^{6}Li, and ^{6}Be, and the 3^+ and 0^+ excited states of ^{6}Li have been accurately calculated with the Green's function Monte Carlo method using realistic models of two- and three-nucleon interactions. The splitting of the $A = 3$ isospin $T = \frac{1}{2}$ and $A = 6$ isospin $T = 1$, $J^\pi = 0^+$ multiplets is also studied. The observed energies and radii are generally well reproduced, however, some definite differences between theory and experiment can be identified.

PACS numbers: 21.10.Dr, 21.45.+v, 21.60.Ka, 27.10.+h

A system of interacting nonrelativistic nucleons is the simplest model of nuclei. Even in this simple model exact calculations have been possible only for a limited number of light nuclei due to the strong spin-isospin dependence of nuclear forces. For many years, only two-nucleon states could be exactly calculated. Next, the Faddeev method was used to study the three-nucleon states [1,2]. In the past decade, many advances have become possible due to the development of supercomputers. Quantum Monte Carlo methods were used to study nuclei with $A \leq 5$ [3,4], the ^{4}He ground state was calculated with the Faddeev-Yakubovosky method [5], and methods using hyperspherical functions were developed to study low-energy three- and four-nucleon states [6]. In this Letter, we report the first realistic six-nucleon ($6N$) quantum Monte Carlo calculations along with updated results for nuclei with $A \leq 5$. Until now the $A = 6$ nuclei have been mostly treated as three-body systems with an α and two nucleons [7].

It appears possible to extend these calculations to several seven- and eight-nucleon states. Unlike the $A = 2$ to 4 nuclei, the $A = 6$ to 8 nuclei have a spectrum of bound states indicating shell structure and spin-orbit coupling. Exact calculations of these nuclei will be useful to probe the physics of the shell model, to construct realistic models of three-nucleon interactions, and will provide wave functions to study electron-scattering observables and reactions of interest in astrophysics.

The new Argonne v_{18} two-nucleon interaction [8] is used here. It is expressed as a sum of four parts:

$$v_{18} = v_{14} + v_{\rm cib} + v_{\rm csb} + v_{\rm em}\,. \tag{1}$$

Its dominant part v_{14} contains 14 isoscalar operators as in the old Argonne v_{14} [9]. The charge-independence-breaking part $v_{\rm cib}$ has three isotensor terms with operators $[3\tau_{iz}\tau_{jz} - \boldsymbol{\tau}_i \cdot \boldsymbol{\tau}_j] \otimes [1, \boldsymbol{\sigma}_i \cdot \boldsymbol{\sigma}_j, S_{ij}]$ and includes the effect of the mass difference between charged and neutral pions. The isovector charge-symmetry-breaking part $v_{\rm csb}$ contains the operator $\tau_{iz} + \tau_{jz}$, and the electromagnetic part $v_{\rm em}$ contains Coulomb and magnetic interactions in all pairs. The kinetic energy operator associated with this model has isoscalar and isovector parts denoted by K and $K_{\rm csb}$:

$$K + K_{\rm csb} = -\frac{\hbar^2}{4}\sum_i \left[\left(\frac{1}{m_p} + \frac{1}{m_n}\right)\nabla_i^2 + \left(\frac{1}{m_p} - \frac{1}{m_n}\right)\tau_{iz}\nabla_i^2\right]. \tag{2}$$

Because of its careful treatment of isospin-symmetry-breaking terms, the new Argonne v_{18} model is well suited to study the mass differences between the $T = \frac{1}{2}$, ^{3}He-^{3}H doublet and the $T = 1$, $J^\pi = 0^+$, ^{6}He-^{6}Li-^{6}Be triplet.

Three-nucleon interactions V_{ijk} described with the Urbana model [10] are included in the nuclear Hamiltonian. These contain a two-pion exchange part $V_{ijk}^{2\pi}$ with its strength $A_{2\pi}$ chosen to reproduce the observed binding energies of ^{3}H and ^{4}He, and a phenomenological spin-isospin independent interaction V_{ijk}^{R} of strength U_0 adjusted to obtain the empirical equilibrium density of nuclear matter. In Urbana models IX (VIII) of V_{ijk}, to be used in conjunction with the new v_{18} (old v_{14}), these parameters have values $A_{2\pi} = -0.0293$ (-0.028) and $U_0 = 0.0048$ (0.005) MeV.

The Green's function Monte Carlo (GFMC) calculations [3,4] are carried out with a simpler isoscalar Hamiltonian:

$$\hat{H} = K + \sum_{i<j} v_8(ij) + \sum_{i<j<k} V_{ijk}\,. \tag{3}$$

The interaction $v_8(ij)$ has eight terms, with operators $[1, \boldsymbol{\tau}_i \cdot \boldsymbol{\tau}_j] \otimes [1, \boldsymbol{\sigma}_i \cdot \boldsymbol{\sigma}_j, S_{ij}, \mathbf{L}\cdot\mathbf{S}]$, chosen such that it

 0031-9007/95/74(22)/4396(4)$06.00 © 1995 The American Physical Society

equals the v_{14} in all S and P waves as well as in the $^3D_1$ wave and its coupling to the $^3S_1$. The eigenstates of $\hat{H}$ are computed, and the contributions of all other terms, namely, $v_{14} - v_8, v_{\rm cib}, v_{\rm csb}, v_{\rm em}$, and $K_{\rm csb}$, to the energy eigenvalue are calculated in first order. The error in the binding energy of ^{3}H due to the perturbative treatment of $v_{14} - v_8$ has been estimated by Kamada and Glöckle [11] to be ~0.02 MeV.

Nuclear states are represented by vector functions $\Psi(\mathbf{R})$ whose components $\psi_\alpha(\mathbf{R})$ give the amplitudes for the nucleons, at spatial coordinates $\mathbf{R} = (\mathbf{r}_1, \mathbf{r}_2, \ldots, \mathbf{r}_A)$, to be in spin-isospin state $|\alpha\rangle$. The GFMC calculation of the lowest energy state with quantum numbers $\xi(= J^\pi, T, T_z)$ and energy E_0 starts with an approximate wave function $\Psi_v(\mathbf{R})$ determined from a variational Monte Carlo (VMC) calculation for that state. It yields values of $\Psi(\tau, \mathbf{R}_i(\tau))$, where

$$\Psi(\tau, \mathbf{R}) = \int d\mathbf{R}'\, G(\mathbf{R}, \mathbf{R}', \tau)\Psi_v(\mathbf{R}'), \tag{4}$$

$$G(\mathbf{R}, \mathbf{R}', \tau) = \langle \mathbf{R}| e^{-(\hat{H}-E_0)\tau} |\mathbf{R}'\rangle \tag{5}$$

at configurations $\mathbf{R}_i(\tau)$ distributed with probability $|\Psi_v^\dagger(\mathbf{R})\Psi(\tau, \mathbf{R})|$. Here i labels configurations which number ~10 000. The $e^{-(\hat{H}-E_0)\tau}$ is considered as a product of many small imaginary time steps $e^{-(\hat{H}-E_0)\Delta\tau}$, with $\Delta\tau \sim 0.0001$ MeV^{-1}. Using the small-time limit of the propagator $e^{-(\hat{H}-E_0)\Delta\tau}$, correct up to order $\Delta\tau$, $\Psi(\tau + \Delta\tau, \mathbf{R}_i(\tau + \Delta\tau))$ are stochastically estimated from the known $\Psi(\tau, \mathbf{R}_i(\tau))$. The $G(\mathbf{R}, \mathbf{R}', \tau)$ is taken as

$$G(\mathbf{R}, \mathbf{R}', \tau) = e^{E_0\Delta\tau} I_3(\mathbf{R}) I_2(\mathbf{R}) \exp\left[\frac{-m(\mathbf{R} - \mathbf{R}')^2}{2\hbar^2\Delta\tau}\right] \times I_2(\mathbf{R}') I_3(\mathbf{R}'), \tag{6}$$

$$I_2(\mathbf{R}) = S\prod\left(1 - \frac{\Delta\tau}{2} v_{\mathbf{L}\cdot\mathbf{S},ij}(\mathbf{R})\right)\exp\left[-v_{6,ij}(\mathbf{R})\frac{\Delta\tau}{2}\right], \tag{7}$$

$$I_3(\mathbf{R}) = \left(1 - \frac{\Delta\tau}{2}\sum V^{2\pi}_{ijk}(\mathbf{R})\right)\exp\left[-\sum V^{R}_{ijk}(\mathbf{R})\frac{\Delta\tau}{2}\right], \tag{8}$$

where v_6 and $v_{\rm LS}$ are the momentum independent and dependent components of the v_8 NN interaction. The free particle Green's function is given by the Gaussian and the gradients in $v_{\rm LS}$ operate only on it. The number of spin-isospin states that contribute to the $T = 0(1)$ $6N$ $\Psi(\mathbf{R})$ is 320 (576), and their propagator $e^{-(\hat{H}-E_0)\Delta\tau}$ is a 320 × 320 (576 × 576) complex matrix function. Therefore $6N$ GFMC calculations are numerically very intensive. They were performed on the IBM SP parallel computer at Argonne National Laboratory with 128 nodes operating at ~40 MFlops/node. Propagating 10 000 $6N$ configurations up to $\tau = 0.06$ MeV^{-1} requires ~2000 node hours. In contrast, the ^{4}He ground state wave function $\Psi(\mathbf{R})$ has only 32 spin-isospin states and requires ~100 node hours for a similar calculation.

It is well known that there are no $A = 5$ bound states. The $\frac{3}{2}^-$ and $\frac{1}{2}^-$ resonances in ^{5}He have been studied by n-^{4}He scattering, and the phase shifts in these partial waves have been extracted [12]. The GFMC calculations are carried out for the scattering states with a node at $|\mathbf{r}_\alpha - \mathbf{r}_n| = 12.5$ fm; however, only the interesting part with $|\mathbf{r}_\alpha - \mathbf{r}_n| < 12.5$ fm is retained in the calculation. Assuming that the interaction between α and n is negligible for $|\mathbf{r}_\alpha - \mathbf{r}_n| > 12.5$ fm the true energy of this state can be obtained from the phase shifts [13].

The variational wave functions used in these calculations include spatial and spin-isospin two-body and three-body correlations denoted by $f_c(r_{ij}), U_{ij}$, and U_{ijk} in Ref. [14], and are determined from the isoscalar part of the full Hamiltonian. The uncorrelated wave functions for ^{3}H and ^{4}He are as given in [14], while those for ^{5}He have an additional nucleon in the $(p\,\frac{1}{2})$ or $(p\,\frac{3}{2})$ scattering state. The two extra nucleons in $6N$ states are in optimized superpositions of $(p\,\frac{3}{2})^2$, $(p\,\frac{1}{2}\,p\,\frac{3}{2})$, and $(p\,\frac{1}{2})^2$ states whose radii are constrained to reasonable values. Details of the VMC and GFMC calculations will be published separately.

The transient energy $E(\tau)$, defined as

$$E(\tau) = \frac{\langle\Psi_v|\hat{H}|\Psi(\tau)\rangle}{\langle\Psi_v|\Psi(\tau)\rangle} = \frac{\langle\Psi(\frac{\tau}{2})|\hat{H}|\Psi(\frac{\tau}{2})\rangle}{\langle\Psi(\frac{\tau}{2})|\Psi(\frac{\tau}{2})\rangle}, \tag{9}$$

provides an upper bound which approaches the lowest-energy eigenvalue with quantum numbers ξ in the limit $\tau \to \infty$. The values of $E(\tau)$, calculated from 10 000 configurations for each of the three $6N$ states and 20 000 configurations for ^{4}He are shown in Fig. 1 along with their statistical error estimates. The ^{4}He $E(\tau)$ decreases from the variational energy $E_v = E(\tau = 0)$ by ~1.2 MeV for $\tau \sim 0.02$ MeV^{-1}, and is almost independent of τ thereafter, suggesting that the Ψ_v has ≤2% admixture of states

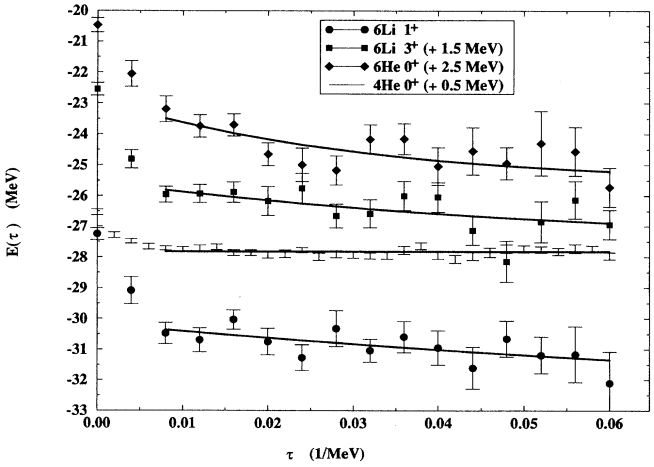

FIG. 1. The top to bottom data sets show the $E(\tau)$ for ^{6}He, ^{6}Li(3$^+$), ^{4}He, and ^{6}Li(1$^+$) states, along with the fits described in the text. Constants of 2.5, 1.5, and 0.5 MeV have been added to the $E(\tau)$ of ^{6}He, ^{6}Li(3$^+$), and ^{4}He, respectively, for clarity.

with excitation energy ≥ 50 MeV. The $E(\tau)$ of the $6N$ states, in contrast, decreases by ~ 4 MeV from E_v, and does not appear to have reached the $\tau \to \infty$ asymptotic value at $\tau = 0.06$ MeV^{-1}. The statistical error, governed by variance of $\hat{H}\Psi_v(\mathbf{R})/\Psi_v(\mathbf{R})$, is larger in the $6N$ $E(\tau)$. These indicate that the $6N$ Ψ_v are not as accurate as the ^{4}He Ψ_v and that they need to be improved for more accurate GFMC calculations.

The average value of $E(\tau)$ in the τ interval 0.03 to 0.06 MeV^{-1} is listed as $\bar{E}$ in Table I. The $\bar{E}$ of ^{3}H, ^{4}He, and ^{5}He can be identified with their ground state energies, however, those of the $6N$ states can only be regarded as upper bounds. It is difficult to extrapolate the $6N$ $E(\tau)$ to $\tau \to \infty$, particularly due to the large statistical errors; nevertheless, we have attempted it in the following way. Let Ψ_i be the eigenstates with quantum numbers ξ and energies E_i. The Ψ_v contains admixtures of Ψ_i with amplitude β_i in addition to the Ψ_0 of the lowest-energy state. Admixtures with the smallest $E_i - E_0$ determine the behavior of $E(\tau)$ at large τ. We approximate the contribution of low-lying states with two delta functions at E_1 and E_2 with amplitudes β_1 and β_2. It is experimentally known that the lowest $T = 0$, $J^\pi = 1^+$ (3^+) resonances in ^{6}Li are 5.65 ($\sim$13.6) MeV above the 1^+ (3^+) bound states [15]. Accordingly, we assume that $E_1 - E_0 =$ 5.65 (13.6) MeV for the 1^+ (3^+) states and, in absence of experimental data, use the value 13.6 MeV also for the $T = 1$, $J^\pi = 0^+$. Further assuming that $E_2 - E_0 =$ 30 MeV the calculated values of $E(\tau > 0.01$ MeV$^{-1})$ are fitted by varying E_0, β_1, and β_2. Fortunately, the fits are not very sensitive to $E_2 - E_0$ and are shown in Fig. 1. The resulting value of E_0 is listed as the calculated energy in Table I. The error in the extrapolated E_0 is much larger than that in $\bar{E}$ and less reliable.

The expectation values of various terms in the Hamiltonian are also listed in Table I. These are averages over the interval $\tau = 0.03$ to 0.06 MeV^{-1}, calculated using

$$\langle \hat{O}(\tau) \rangle = 2\frac{\langle \Psi_v|\hat{O}|\Psi(\tau)\rangle}{\langle \Psi_v|\Psi(\tau)\rangle} - \frac{\langle \Psi_v|\hat{O}|\Psi_v\rangle}{\langle \Psi_v|\Psi_v\rangle}, \qquad (10)$$

correct up to order $|\Psi(\tau)\rangle - |\Psi_v\rangle$. The dominant $\langle v_{14}\rangle$ and $\langle K\rangle$ have similar values in ^{4}He and ^{5}He, while in the $6N$ states they are closer to the sum of their values in ^{4}He and ^{2}H. The $\langle V_{ijk}\rangle$ are similar in ^{4}He, ^{5}He, and $6N$ states. The $\langle v_{\rm LS}\rangle$ contains both $\mathbf{L}\cdot\mathbf{S}$ and $\mathbf{L}\cdot\mathbf{S}(\boldsymbol{\tau}_i\cdot\boldsymbol{\tau}_j)$ terms in the NN interaction. They contribute, along with V_{ijk} [16], to the splitting between $\frac{3}{2}^-$ and $\frac{1}{2}^-$ states of ^{5}He. However, the calculated splitting of 0.8 (3) MeV is much smaller than the observed 1.4 MeV. The magnitudes of $\langle v_{\rm LS}\rangle$ and $\langle V_{ijk}\rangle$ are larger in the $6N$ 0^+ and 3^+ states than in the 1^+, suggesting that the 1^+ has less contribution from the $(p\frac{3}{2})^2$ configuration than the other two. The underbinding of the $6N$ 0^+ and 3^+ states by ~ 1 MeV is probably related to that of the ^{5}He $\frac{3}{2}^-$ state. In ^{5}He, only the expectation value $\langle v_{\rm Coul}^{pp}\rangle$ of the Coulomb interaction between protons is calculated. The other terms in $\langle v_{\rm em}\rangle$ for ^{5}He (given in parentheses in Table I) are taken from VMC calculations. The $\langle v_{\rm Coul}^{pp}\rangle$ decreases by $\sim 5\%$ from ^{4}He to ^{6}He, indicating that the α cluster expands as we go from $A = 4$ to 6.

The last three lines of Table I give rms proton and neutron radii. The calculated values of $R(p)$ compare well with the those extracted from observed charge radii [17]. The experimental $R(p)$ of ^{3}He is 1.77 fm, in reasonable agreement with the calculated $R(n)$ of ^{3}H. The Coulomb interaction accounts for most of the isovector ^{6}Be-^{6}He difference (Table II). Since this difference is correctly predicted, the $R(p)$ of ^{6}Be, assumed to be equal to the $R(n)$ of ^{6}He, appears to have a reasonable value.

The contributions of $v_{\rm em}, v_{\rm cib}, v_{\rm csb}$, and $K_{\rm csb}$, treated as first order perturbations in this work, are responsible for the energy differences within the $T = \frac{1}{2}$ $3N$ and $T = 1$, $J^\pi = 0^+$ $6N$ multiplets listed in Table II. The present Hamiltonian explains the isovector energy differences ^{3}He-^{3}H and ^{6}Be-^{6}He fairly well. The three-body calculations show that the isovector $v_{\rm csb}$ and $K_{\rm csb}$ are necessary to obtain the observed ^{3}He-^{3}H difference, in agreement with earlier results of Faddeev calculations [18]. Unfortunately, the calculated value of the isotensor difference $\frac{1}{2}$ (^{6}Be + ^{6}He)-^{6}Li is much larger than observed.

TABLE I. Calculated energies and radii in MeV and fm.

Nucleus (J)	^{2}H(1)	^{3}H($\frac{1}{2}$)	^{4}He(0)	^{5}He($\frac{3}{2}$)	^{5}He($\frac{1}{2}$)	^{6}He(0)	^{6}Li(1)	^{6}Li(3)
E (Expt.)	−2.22	−8.48	−28.3	−27.2	−25.8	−29.3	−32.0	−29.8
E (Calc.)	−2.22	−8.47(2)	−28.3(1)	−26.5(2)	−25.7(2)	−28.2(8)	−32.4(9)	−28.9(6)
$\bar{E}$	−2.22	−8.47(2)	−28.3(1)	−26.5(2)	−25.7(2)	−27.3(4)	−31.1(4)	−28.2(3)
$\langle K\rangle$	19.9	50.0(1)	118.0(1)	122.0(2)	117.0(2)	146.0(4)	143.0(3)	138.0(3)
$\langle v_{14}\rangle$	−22.1	−58.0(1)	−142.0(1)	−145.0(2)	−140.0(2)	−172.0(4)	−173.0(3)	−165.0(3)
$\langle V_{ijk}\rangle$	0	−1.20(3)	−6.5(3)	−7.0(4)	−6.4(4)	−7.0(7)	−6.2(6)	−6.9(5)
$\langle v_{\rm LS}\rangle$	−0.08	−0.20(5)	−0.4(1)	−1.2(1)	−0.4(1)	−2.7(3)	−1.5(5)	−3.0(4)
$\langle v_{\rm em}\rangle$	0.018	0.039(1)	0.879(5)	(0.87)	(0.87)	0.87(1)	1.71(2)	1.72(2)
$\langle v_{\rm Coul}^{pp}\rangle$	0	0	0.761(2)	0.745(3)	0.751(3)	0.724(8)	1.55(2)	1.57(2)
$R(n)$	1.967	1.72	1.42(1)	3.02(3)	3.57(3)	2.62(1)	2.41(5)	2.46(7)
$R(p)$	1.967	1.58	1.42(1)	1.84(2)	1.99(2)	1.89(6)	2.41(5)	2.46(7)
$R(p)$ (Expt.)	1.953	1.61	1.47				2.43	

TABLE II. Energy differences in MeV within isospin multiplets.

	^{3}He-^{3}H	^{6}Be-^{6}He	$\frac{1}{2}(^6\text{Be} + {}^6\text{He})$-^{6}Li
$\langle v_{\text{em}} \rangle$	0.677	2.33	0.33
$\langle K_{\text{csb}} \rangle$	0.014	0.036	0
$\langle v_{\text{csb}} \rangle$	0.066	0.116	0
$\langle v_{\text{cib}} \rangle$	0	0	0.28
Δ (Calc.)	0.757(1)	2.5(1)	0.6(1)
Δ (Expt.)	0.764	2.35	0.34

The observed difference is essentially explained by the electromagnetic interaction alone. This is very puzzling because most of the contribution of the isotensor v_{cib} to this difference should be from the relative $^1S_0$ two-nucleon state in which the difference between pp and np phase shifts seems to be well established [19,20]. The nonperturbative contribution of the Coulomb interaction, particularly in ^{6}Be, neglected here, may reduce the value of this isotensor difference. There could also be some contribution from charge dependence of the two-pion exchange V_{ijk}.

In conclusion, we have demonstrated that the GFMC method can be used to accurately calculate the energies of the many nuclear states with $A \leq 6$ from realistic models of nuclear forces. The calculated energies are in good agreement with experiment. However, some differences, such as the underestimation of the splitting between $\frac{3}{2}^-$ and $\frac{1}{2}^-$ states of ^{5}He are clearly established. We could attempt to probe relativistic effects [21,22], and the spin-isospin dependence of the short-range part of the V_{ijk} using these differences. A detailed analysis of the GFMC wave function $e^{-\hat{H}\tau}\Psi_v$ is in progress to study the structure of the $6N$ states and improve upon their Ψ_v.

The $6N$ calculations were made possible by a generous grant of computer time from the Mathematics and Computer Science Division of Argonne National Laboratory. We also received valuable support from the National Energy Research Supercomputer Center at Livermore and the National Center for Supercomputing Applications at Urbana. The authors thank Dr. Steven C. Pieper for many useful suggestions. The work of B. S. P. and V. R. P. is supported by the U.S. National Science Foundation via Grant No. PHY89-21025, that of J. C. by the U.S. Department of Energy, and that of R. B. W. by the U.S. Department of Energy, Nuclear Physics Division, under Contract No. W-31-109-ENG-38.

[1] C. R. Chen, G. L. Payne, J. L. Friar, and B. F. Gibson, Phys. Rev. C **31**, 2266 (1985).
[2] W. Glöckle, H. Witala, and Th. Cornelius, Nucl. Phys. **A508**, 115C (1990).
[3] J. Carlson, Phys. Rev. C **38**, 1879 (1988); Nucl. Phys. **A508**, 141c (1990); **A522**, 185c (1991).
[4] J. Carlson and R. Schiavilla, in *Few Body Systems Suppl. 7,* edited by B. L. G. Bakker and R. van Dantzig (Springer-Verlag, Wien, 1994), p. 349.
[5] W. Glöckle and H. Kamada, Phys. Rev. Lett. **71**, 971 (1993).
[6] A. Kievsky, M. Viviani, and S. Rosati, Nucl. Phys. **A551**, 241 (1993); **A577**, 511 (1994).
[7] N. W. Schellingerhout, L. P. Kok, S. A. Coon, and R. M. Adam, Phys. Rev. C **48**, 2714 (1993), and references therein.
[8] R. B. Wiringa, V. G. J. Stoks, and R. Schiavilla, Phys. Rev. C **51**, 38 (1995).
[9] R. B. Wiringa, R. A. Smith, and T. L. Ainsworth, Phys. Rev. C **29**, 1207 (1984).
[10] J. Carlson, V. R. Pandharipande, and R. B. Wiringa, Nucl. Phys. **A401**, 59 (1983).
[11] H. Kamada and W. Glöckle (private communication).
[12] R. A. Arndt and L. D. Roper, Nucl. Phys. **A209**, 447 (1973).
[13] J. Carlson, V. R. Pandharipande, and R. B. Wiringa, Nucl. Phys. **A424**, 47 (1984).
[14] R. B. Wiringa, Phys. Rev. C **43**, 1585 (1991).
[15] F. Ajzenberg-Selove, Nucl. Phys. **A413**, 1 (1984).
[16] S. C. Pieper and V. R. Pandharipande, Phys. Rev. Lett. **70**, 2541 (1993).
[17] H. De Vries, C. W. De Jager, and C. De Vries, At. Data Nucl. Data Tables **36**, 495 (1987).
[18] Y. Wu, S. Ishikawa, and T. Sasakawa, Phys. Rev. Lett. **64**, 1875 (1990); **66**, 242 (1991).
[19] J. R. Bergervoet, P. C. van Campen, R. A. M. Klomp, J.-L. de Kok, T. A. Rijken, V. G. J. Stoks, and J. J. de Swart, Phys. Rev. C **41**, 1435 (1990).
[20] V. G. J. Stoks, R. A. M. Klomp, M. C. M. Rentmeester, and J. J. de Swart, Phys. Rev. C **48**, 792 (1993).
[21] G. E. Brown, W. Weise, G. Baym, and J. Speth, Comments Nucl. Part. Phys. **XVII**, 39 (1987).
[22] J. Carlson, R. Schiavilla, and V. R. Pandharipande, Phys. Rev. C **47**, 484 (1993).